Journal of Structural Geology, Vol. 7, No. 2, pp. 175 to 186, 1985
Printed in Great Britain

0191–8141/85 $03.00 + 0.00
© 1985 Pergamon Press Ltd.

Microtectonic evidence for eastward ductile shear in the Jurassic orogen of SW Japan

MICHEL FAURE*

Laboratoire de Géologie Structurale, C.N.R.S. L.A. 215. Orléans University, France

(*Received* 23 *March* 1984; *accepted in revised form* 6 *August* 1984)

Abstract—Two Jurassic deformation phases are responsible for the thrust and nappe structures in the infrastructure of the outer belt of the Mesozoic chain of SW Japan. The first phase was synmetamorphic, and took place under HP/LT conditions. Microtectonic analysis shows that the penetrative deformation corresponded to a ductile shear directed from W to E, parallel to the stretching and mineral lineation. At the regional scale the first phase corresponded to the obduction of the Greenschist nappes upon the Kurosegawa continent. During the second phase the Greenschist nappes were sliced, leading to an apparent reverse metamorphic zoning. The first phase structures were then locally reworked by folds giving rise to an apparent westwards sense of shear.

INTRODUCTION

THE PRESENT island arc of Japan is overprinted upon a polyorogenic chain formed during three orogenic cycles. From younger to older these are: the early Tertiary Shimanto orogeny, the late Jurassic orogeny, partly similar to the early stages of the Sakawa Orogeny of Kobayashi (1941) and the late Paleozoic Akiyoshi Orogeny.

The late Jurassic orogeny, discussed in this paper, affects all SW Japan except its southernmost part or Shimanto zone, whose structure was caused by the Shimanto orogeny. It is divided into outer and inner belts (respectively on the Pacific Ocean and Japan Sea sides) by the Median Tectonic Line (MTL) a polyphase strike-slip fault whose earlier left-lateral motion occurred in Middle Cretaceous time (Ichikawa 1980, fig. 1). The outer belt is classically divided into parallel zones bounded by late faults (e.g. Kimura 1973, Tanaka & Nozawa 1977).

The dominant tectonic style, however, is *tangential*, a term used in this paper for a tectonic style in which horizontal displacements predominate over vertical ones, and characterized by flat-lying thrusts and nappes. For this reason, the Jurassic chain is better divided into superstructure and infrastructure (Faure 1984). The infrastructure is characterized by polyphase tectonometamorphism. Though the HP/MT Sanbagawa metamorphism is world famous (e.g. Miyashiro 1961, Iwasaki 1963, Banno 1964, Ernst *et al.* 1970), the related deformation structures were studied by Hide *et al.* (1956), Hide (1961, 1972), Kawachi (1968), Hara *et al.* (1977), Takasu & Makino (1980), Research Group of the Sanbagawa Belt (1981), Shiota (1981) and Toriumi (1982). However the nature of the tectonic movement during the main phase of metamorphism has only been studied recently (Faure 1982). This paper aims to describe the ductile deformation and to link it with the large-scale thrusting of oceanic sediments; and thus to provide a new example showing that plurikilometric tangential structures can be reliably understood by microstructural analysis.

THE GEOLOGICAL FRAMEWORK

Four paleogeographic domains defined in Shikoku island (Faure 1984) (Figs. 2 and 3), form the outer belt of the Jurassic orogen.

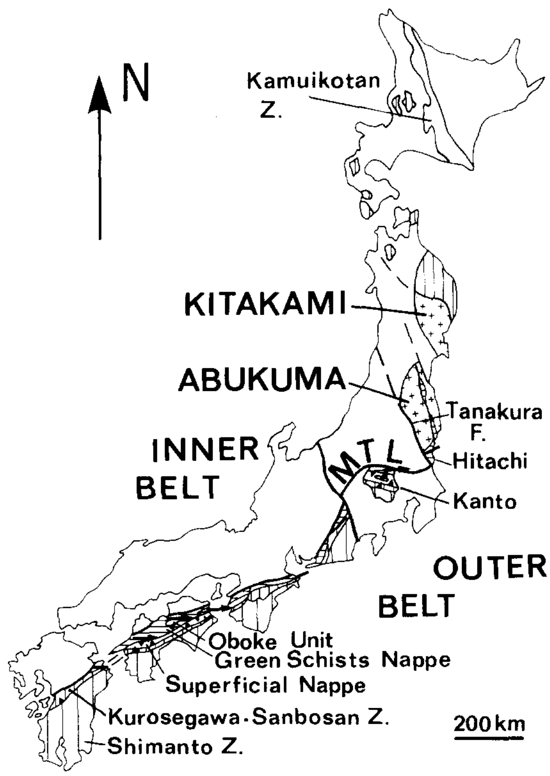

Fig. 1. General situation of the outer belt of SW Japan. The Kurosegawa zone and the Sanbosan zone are grouped together. MTL, Median Tectonic Line.

* Present address: Department of Earth Sciences, Kyoiku-gakubu, Tokushima University; 770 Tokushima. Japan.

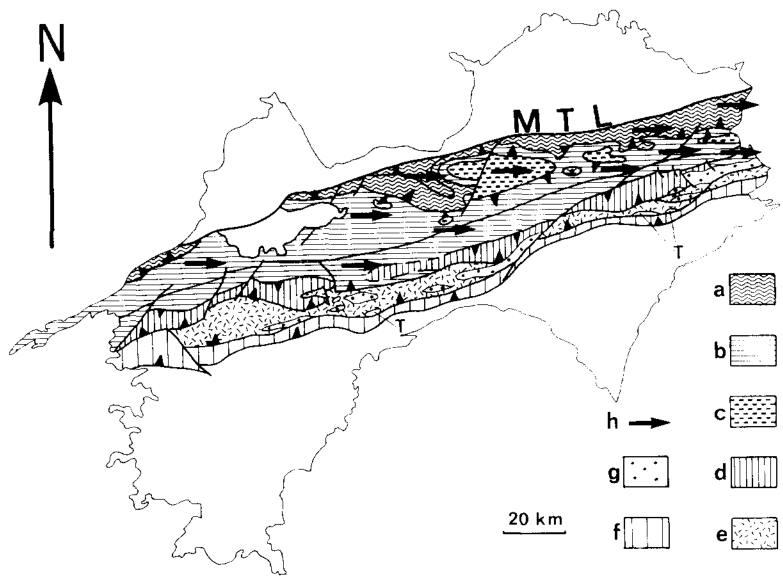

Fig. 2. Structural map of Shikoku. (a,b) Greenschist nappes; (a) highly metamorphic Mt. Kotsu nappe; (b) epimetamorphic Shozanji nappe. (c)–(e) Kurosegawa continent; (c) Oboke sandstone rich unit; (d) superficial nappe (Middle Jurassic olistostrome); (e) Kurosegawa zone (crustal rocks); (f) Sanbosan zone, late Jurassic flysch; (g) unconformable Neocomian deposits; (h) average L_1 with eastward sense of shear; T, Triassic. (a)–(c) Infrastructure; (d)–(f) superstructure; MTL, Median Tectonic Line.

A superficial nappe

This consists of a middle Jurassic olistostrome thrust up southwards from the north of the MTL, during late Jurassic time (Faure & Charvet 1983).

The Greenschist nappes

These are composed of pelitic schist, radiolarite and basic schist. Conodonts from calcschist associated with basic schist provide late Triassic ages (Matsuda 1978), and the upper part of the sedimentary pile probably reaches the middle Jurassic in view of findings of ill preserved radiolaria (Suyari *et al.* 1982). The basic and ultramafic rocks have been regarded as ophiolites; but it is now established that the igneous rock-types (pillow lava, diabase, gabbro and rare ultramafic rocks) are olistoliths enclosed in green sediments: shale, breccia and sandstone containing reworked gabbroic minerals (Iwasaki 1979). Pretectonic ophiolitic detritus occurs at the present day in a variety of environments: rifts, marginal seas, fracture zones or ridges like the Goringe bank, where it has been observed *in situ* (Lagabrielle *et al.* 1982). An intraoceanic sedimentary environment is therefore tentatively proposed for the Greenschist nappes.

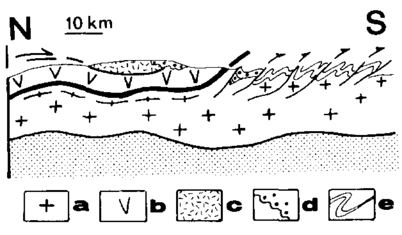

Fig. 3. Schematic cross-section of the outer part of the Jurassic orogen at the scale of the crust, omitting Tertiary granites. (a) Kurosegawa basement, deformed near the nappe contact; (b) Greenschist nappes (undifferentiated); (c) superficial nappe; (d) unconformable Neocomian deposits; (e) Late Jurassic Sanbosan flysch and Cretaceous North Shimanto flysch. Stipple tone, mantle.

The Kurosegawa basement

This crops out along a post Cretaceous strike-slip fault called the Kurosegawa tectonic zone (Ichikawa *et al.* 1956, Hada *et al.* 1979, Maruyama 1981). Because serpentinite associated with 400 Ma metamorphic rocks acts as a soft medium and wraps around the other rocks, the Kurosegawa tectonic zone is often seen as a serpentinite mélange. The lithologic succession before the strike-slip movement can be reconstructed. It comprises Devonian granitoids. Paleozoic metamorphic rocks and sediments unconformably covered by Triassic and Jurassic shallow-water sediments. These rocks represent fragments of a microcontinent underlying the Greenschist nappes, and are referred to here as the Kurosegawa basement. Northwards, an early Jurassic sandstone–mudstone formation includes olistoliths of Paleozoic rocks derived from the Kurosegawa basement, and of late Triassic radiolarites and basic schist similar to the formations of the Greenschist nappes (Fig. 4). This formation, called the Ultra-Kurosegawa zone (Faure 1984), is interpreted as a transitional domain between the Greenschist nappes and the underlying Kurosegawa basement. In Central and Eastern Shikoku, the Greenschist nappes have been thrust onto the Oboke Unit, which consists of pelitic schist; sandstone with zircon, tourmaline, and apatite; and conglomerate with pebbles of acid lava and granite. Undated chert and basic schist are also present as olistoliths. From facies similarities, the Oboke Unit is interpreted as a northward metamorphosed and deformed extension of the Ultra-Kurosegawa zone. According to Kojima (1973)

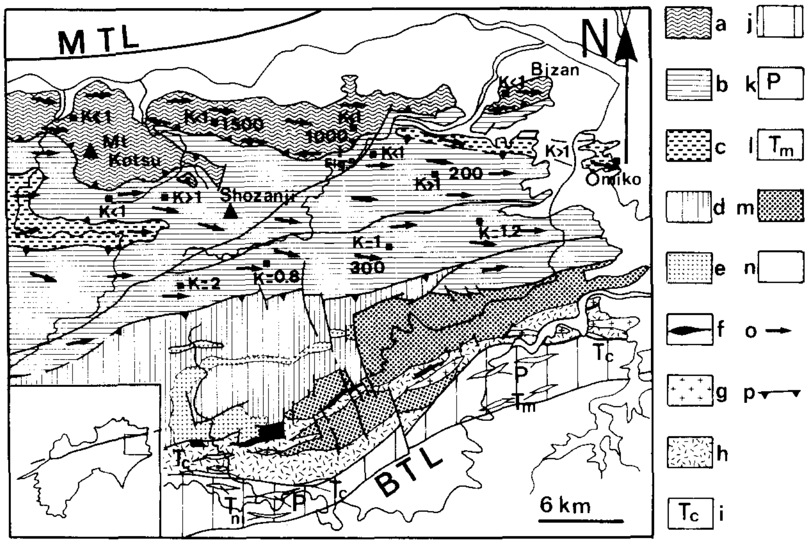

Fig. 4. Structural map of Eastern Shikoku. (a) Mt. Kotsu nappe; (b) Shozanji nappe; (c) Oboke unit; (d) superficial nappe; (e) olistoliths of Late Paleozoic basic rocks; (f) serpentinite; (g) Kurosegawa granites; (h) Kurosegawa Paleozoic sediments; (i) detrital Triassic sediments (Tc) upon the Kurosegawa rocks; (j) Late Jurassic Sanbosan flysch; (k) Late Paleozoic Kurosegawa rocks (P) reworked into the flysch; (l) Triassic olistoliths (Tm); (m) shallow water Neocomian sandstone and conglomerate; (n) Cretaceous Shimanto zone south of the BTL; (o) first phase stretching lineation (L_1) parallel to the maximum extension axis X. Numbers are the maximum extension in %, K is the Flinn parameter. Extension values are from radiolarians; $K < 1$, $K > 1$ are deduced from pressure shadows along Y axis; (p) thrust. MTL, Median Tectonic Line; BTL, Butsuzo Tectonic Line.

the sedimentology of the conglomerates shows that they were supplied from a southern area. This hypothesis fits with the seismic data (Kimura & Okano 1980) supporting the existence of a crust of sialic type south of the MTL.

The South Kurosegawa basin or Sanbosan zone

This is made of middle-late Jurassic flysch including late Paleozoic and early Mesozoic olistoliths. The Sanbosan zone is bounded to the south by a fault: the Butsuzo Tectonic Line. Together with the Cretaceous flyschs of the Shimanto zone, the Sanbosan zone and the fault are unconformably covered by Neocomian shallow water deposits.

The superficial nappe, the Kurosegawa basement, and the South Kurosegawa zone belong to the superstructure while the Greenschist nappes and the Oboke Unit belong to the infrastructure. The structure of the Jurassic orogen is due to two tangential tectonic phases followed by a phase of upright folding as described below. During the first phase, present only in the infrastructure, the Greenschist nappes were thrust eastwards upon the Kurosegawa continent under ductile, synmetamorphic conditions. During the second phase, in late Jurassic time, the middle Jurassic olistostrome (which lacks the first-phase deformation structures) was thrust into the superstructure and the infrastructure was reworked under more superficial conditions.

THE POLYPHASE DEFORMATION OF THE INFRASTRUCTURE

The infrastructure suffered from younger to older the following brittle and ductile deformations.

Paleocene faulting

This has not been studied in detail. Two directions, NE–SW and SSW–NNE, of strike-slip faults are recognized. Their left-lateral motion is related to the brittle deformation stages of the MTL (Ichikawa 1980).

Cretaceous upright folding

This third phase of folding is responsible for the kilometre-scale antiforms and synforms (F_3 folds), trending E–W (N80°E–N110°E). At the outcrop scale, the F_3 folds bear a subvertical fan-shaped crenulation cleavage. According to Hara *et al.* (1977), the F_3 folds are arranged in a left-handed, en-échelon disposition, probably related to the left-lateral motion along the MTL.

The second phase of folding

This is characterized by asymmetric folds (F_2) with gently dipping axial planes and axes trending N90°E–N120°E, with a fan-shaped crenulation cleavage (Fig. 5).

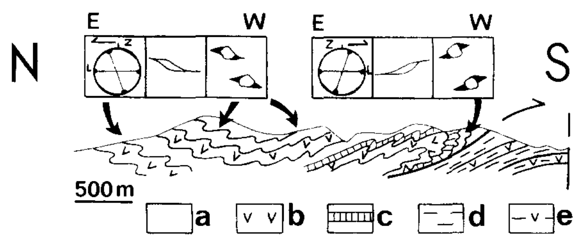

Fig. 5. Schematic cross section of the basal thrust of the Mt. Kotsu nappe (second phase) in Eastern Shikoku (location in Fig. 4). (a)–(c) Mt. Kotsu nappe; (a) pelitic schist; (b) basic schist; (c) radiolarites. (d and e) Shozanji nappe; (d) pelitic schist; (e) basic schist. Adjacent to the thrust zone, drag folds invert both the foliation and the first phase E-directed rotational criteria, producing apparent westward asymmetry.

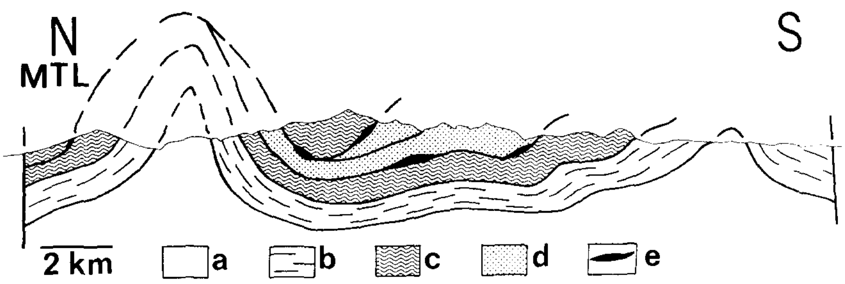

Fig. 6. Cross-section of the infrastructure in Central Shikoku (location in Fig. 7). (a) Oboke unit; (b) Shozanji nappe. (c)–(e) Mt. Kotsu nappe; (c) garnet zone; (d) biotite zone; (e) serpentinite bodies. MTL, Median Tectonic Line.

Statistically they show a southward apparent overturning, and where recrystallization is not so intense, for instance in the southernmost part of the Greenschist nappes, graded bedding allows determination of a southward facing for the second phase. It is uncertain, however, whether or not the rocks were already inverted during the first phase. This second phase is responsible for two main nappe structures (Figs. 2 and 4). In the superstructure there is the emplacement of the Middle Jurassic olistostrome. In the infrastructure there is the slicing of the first-phase Greenschist nappe into two units, causing the apparent metamorphic inversion. These units are (a) the Mt. Kotsu nappe, with biotite–garnet schist, glaucophane schist and amphibolite, which has been thrust upon (b) the Shozanji nappe, made up of low-grade pelitic schist and pumpellyite–actinolite basic schist. The contact zone of approximately 500 m thickness is marked by flat lying brittle shear zones and drag folds showing a southward displacement well observed in Eastern Shikoku (Faure 1983) (Fig. 5). In Central Shikoku, the existence of large-scale second-phase recumbent folds has been assumed based on the asymmetry of microfolds (Hide *et al.* 1956, Hide 1972, Kawachi 1968, Ernst *et al.* 1970) and reverse metamorphic zoning (Banno *et al.* 1978). This model has been extended westwards (Hide 1972) and eastwards (Hara *et al.* 1977, Shiota 1981). But it has been recently questioned in Central Shikoku by Takasu & Makino (1980), who state that there is no evidence for the recumbent folding, all the rocks belong to the same sedimentary sequence, and the biotite crystallization is related to a kind of contact metamorphism caused by the mafic masses, which they regard as intrusions. The locations of the recumbent syncline and anticline axes differ for each author. The second-phase structures can be better explained as in Eastern Shikoku, by a stacking of thrust nappes, each including rocks of different metamorphic grade, separated by shear zones parallel to the foliation (Figs. 6 and 7).

The first phase of deformation

This was contemporaneous with the HP/MT Sanbagawa metamorphism and produced conspicuous penetrative microstructures such as foliation, lineation, and folds, described below. At the regional scale, two kinds of tangential contacts are attributed to the first phase. Inside the Mt. Kotsu nappe, there are several ductile shear zones, containing mylonitized serpentinite pods and actinolite nodules. As there is no metamorphic gap

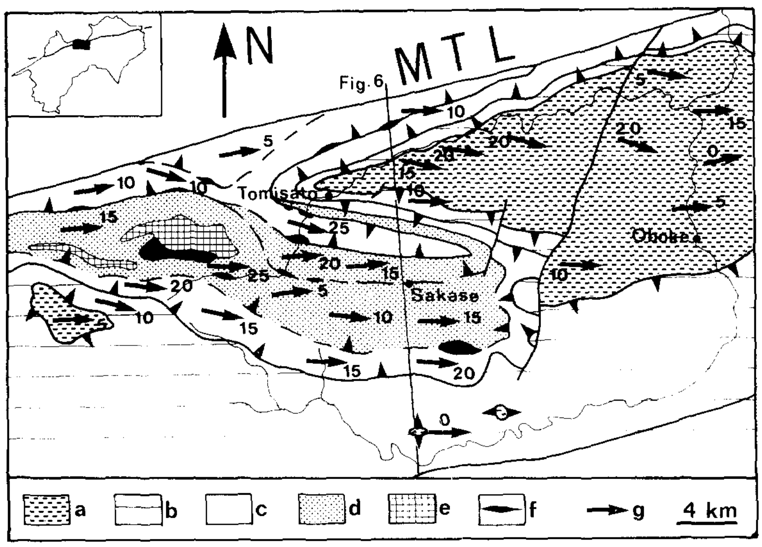

Fig. 7. Structural map of the infrastructure in Central Shikoku. (a) Oboke sandstone unit. (b) Shozanji nappe (epimetamorphic schist). (c)–(f) Mt. Kotsu high grade schist; (c) garnet zone; (d) biotite zone; (e) amphibolite bodies; (f) serpentinite bodies; (g) L_1 lineations. Each location represents average of about 15 field observations, numbers are the plunge, arrows show the sense of rotation. MTL, Median Tectonic Line.

across the contact and the first-phase microstructures are observed on both sides of the shear zone, they are attributed to the first phase, but a late reworking is also possible. Moreover, as the serpentinites are olistoliths, they provide a lithological discontinuity with the sediments, promoting further slip and fluid circulation.

The contact between the Oboke unit and the Shozanji nappe is not always clearly observed, as the rocks are of the same metamorphic grade on both sides; but it is marked in Eastern and Central Shikoku by crushed zones with intense microfolding and quartz veins. There also, a late reworking is likely. The three phases (F_1, F_2 and F_3) of folds are nearly homoaxial and do not allow a sharp phase separation using the trend of the microfolds. The homoaxiality can be explained by the anisotropy created by the first phase lineation, which created an easier deformation direction for the following deformation phases.

THE SANBAGAWA METAMORPHISM

The Sanbagawa metamorphism has long been studied by means of isograd mapping and considerations of phase transitions and P/T conditions (e.g. Miyashiro 1961, Iwasaki 1963, Banno 1964, Ernst *et al.* 1970, Higashino 1975, Banno *et al.* 1978). The Sanbagawa metamorphism is of plurifacial high-pressure intermediate-temperature type, but with atypical features; for instance the HP phases such as jadeite + quartz, lawsonite and aragonite are lacking and the glaucophane–schist outcrops are geographically limited. From the study of mineral associations in pelitic schist, the chlorite, garnet and biotite zones are defined for the prograde stages of metamorphism (Higashino 1975). The prograde stage is afterwards followed by a retrogressive one marked by chlorite and actinolite crystallization (Fig. 8). The mafic and ultramafic masses included in the pelitic schist show a more complex history (Yokoyama 1980). Before the Sanbagawa metamorphism, some masses suffered a granulitic metamorphism at about 750°C, 5–10 kbar. Then during the Sanbagawa metamorphism they reached the amphibolite facies, and even in some areas the eclogite field with estimated P/T conditions about 600°C, 8 kbar.

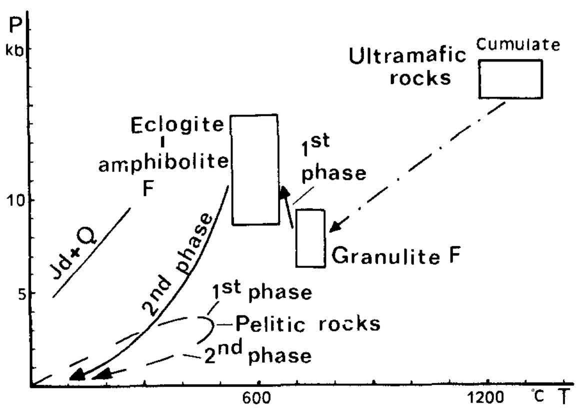

Fig. 8. P–T path of pelitic rocks (stippled line) and ultramafic rocks (boxes); modified from Yokoyama 1980.

THE FIRST-PHASE MICROSTRUCTURES

The first-phase microstructures are the foliation (S_{0-1}), the lineation (L_1) and the isoclinal folds (F_1). They are conspicuous in the infrastructure and in contrast to the second- and third-phase features, they are penetrative from the scale of the thin section to the regional one.

Foliation and lineation

The foliation is the main reference surface, and in the Mt. Kotsu nappe is marked by the preferred orientation of phyllosilicates and quartzo-feldspathic ribbons. In the low metamorphic grade area, sedimentary structures are commonly preserved. Thus, S_{0-1} corresponds to a bedding-foliation surface. S_{0-1} bears a conspicuous L_1 lineation defined by mineral preferred orientation (L_{1m}), stretching lineation (L_{1e}) and fold axes (L_{1f}). The L_1 general trend is around N70°E–N100°E, that is to say E–W on average (Figs. 4 and 7). However some noticeable deviations occur, especially in highly folded areas of limited extent, probably related to curviplanar folds. L_{1m} corresponds to crystallization or recrystallization of minerals as such as amphibole and tourmaline needles, albite porphyroblasts, and quartz and chlorite fibres in pressure shadows. Elongate structures (L_{1e}) formed by by ductile or brittle deformation mechanisms are conspicuously visible at all scales. At the hand sample and outcrop scale, they include for example elongate pillow-structures and vesicles in lava, prolate pebbles in breccia and stilpnomelane boudins in basic schist. In thin-section brittle features include pull-apart structures and comminution of strain-resistant minerals such as garnet, tourmaline, amphibole, epidote, piedmontite and pyroxene, as reported by Toriumi (1982). Stretching due to ductile strain is observed in quartz grains in sandstone, vesicles in lava, radiolaria in chert and quartz ribbons in highly metamorphosed rocks. Fold axes, crenulations, and microwrinkles parallel to L_{1m} strengthen the linear fabric. Generally, the rock fabric is $S > L$, but $L > S$ tectonites, produced by a high concentration of fold hinges or prolate pebbles, occur locally.

Folding

The folds related to the first deformation phase are divided into three groups based on their geometry. The F_{1a} fold-type is the most common. They are metric to millimetric isoclinal folds observed in all kinds of rocks (Fig. 9). The F_{1b} type is more scanty, but always associated with the F_{1a} type, and is common in quartz-schist, calc-schist and glaucophane–epidote schist. They present the classical eye or mushroom-shaped sections characteristic of sheath folds (e.g. Carreras *et al.* 1977, Quinquis *et al.* 1978, Faure & Malavieille 1980, Mattauer *et al.* 1981) (Figs. 10 and 15). Indeed, the F_{1a} and F_{1b} types are probably two different aspects of the same fold style, but this cannot be verified where three-dimensional exposures are lacking. The F_{1c} fold-type occurs

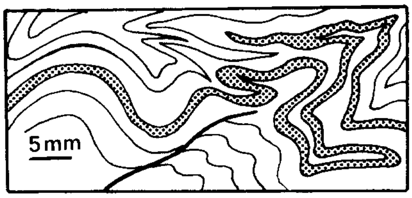

Fig. 9. Isoclinal F_{1a} fold refolded by F_2 fold, marked by quartz veins in pelitic schist (stippled). Such folds are common in pelitic schists but seldom observed because of a lack of appropriate markers.

only in well-banded pelitic schist. They are curviplanar folds, as shown by curved axes and the wide scattering of axes and intersection lineations in the S_{0-1} plane (Figs. 11 and 15), while the L_1 lineation keeps the same E–W trend. The S_{0-1} planes appear to have behaved as a shear-plane, at least in the late stages of the first phase. According to experiments (Cobbold & Quinquis 1980), and other natural examples (e.g. Carreras *et al.* 1977, Faure & Malavieille 1980), sheath and curviplanar folds are formed in ductile shear zones during progressive simple shear. In the case of F_{1c} fold type, it seems that a more complex mechanism occurred involving discontinuous slip on the S_{0-1} surface. These features suggest that the F_1 folds were probably formed during a shear deformation. This hypothesis will be tested by the analysis of the strain ellipsoid and the deformation regime.

Strain ellipsoid

The principal strain axes ($X > Y > Z$) are qualitatively related to rock fabric, following Flinn. The maximum flattening plane XY corresponds to S_{0-1} and the maximum extension axis X is parallel to L_1. This does not fit with the previous statement that S_{0-1} acted also locally as a shear plane during the formation of the F_{1c} folds. But the slip along S_{0-1} probably occurred in the last stages of the first phase, and the discrepancy can be explained if one considers that for high shear strains the angle between the shear plane and the maximum flattening plane is very small and hence cannot be precisely measured. Previous measurements of conglomeratic schist in the Oboke area provide an oblate strain ellipsoid (Hara *et al.* 1973). In the Kanto mountains, Toriumi (1982) found that the maximum extension of deformed radiolarians is parallel to the mineral lineation and the longitudinal strain changes from 5 to 2000% with increasing temperature. Similar results were found in Eastern Shikoku (Fig. 4). In the southern part of the Shozanji nappe, where the metamorphic grade is weak, radiolarians were used as strain markers, because they can be assumed to be close to a sphere in the undeformed state. The shape parameter $K = (X/Y - 1)/(Y/Z - 1)$ is close to 1. In higher metamorphic grades, radiolarians are difficult to recognize. The longitudinal strain, e, is inferred from pull-apart structures in brittle minerals such as pyroxene, amphibole, piedmontite and garnet, using the relation $e = (l - lo)/lo$ where lo and l are the initial and present lengths of the marker, respectively. But the measured strain is probably underestimated because the host rocks deform more than the included strain resistant minerals. A qualitative estimate of the strain ellipsoid is provided by pressure shadows in YZ sections (Choukroune & Lagarde 1977). Where crystallization fibres develop along the Y axis, this direction is an extension axis as well as X. The strain ellipsoid then falls into the oblate field, $K < 1$.

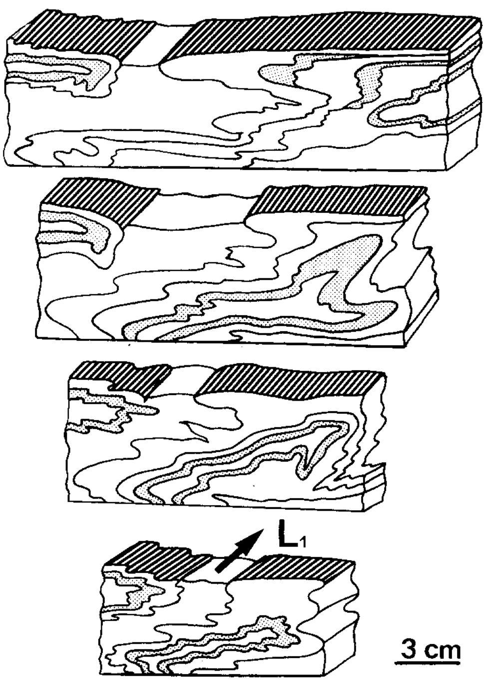

Fig. 10. Serial cross sections of sheath folds (F_{1b}) in epidote–glaucophane schist. Mt. Kotsu nappe, SE of Mt. Kotsu.

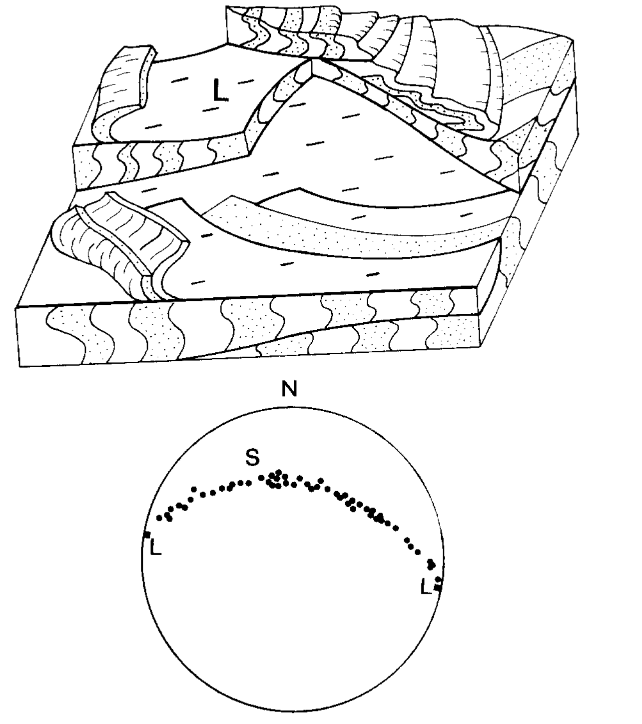

Fig. 11. Schematic block diagram of F_{1c} curviplanar folds (cf. Fig. 14). During shear, the axes are progressively reoriented parallel to the stretching lineation, L. The diagram shows the scattering of axes within the schistosity plane (50 measurements, Oboke Unit, Omiko).

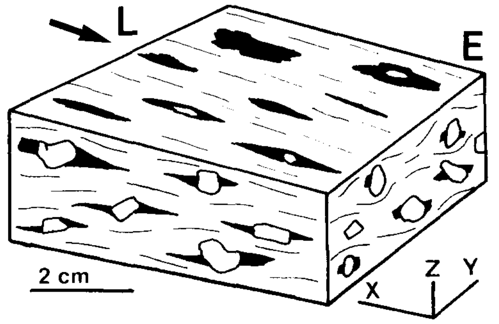

Fig. 12. Schematic block diagram of hand-specimen hyaloclastite with $S > L$ tectonic fabric and asymmetric pressure shadows in XZ sections at the end of magmatic porphyroclasts (Shozanji nappe, W of Omiko).

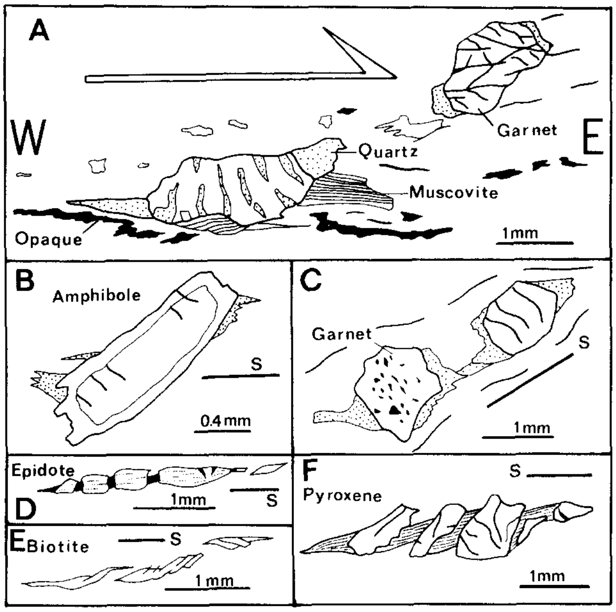

Fig. 13. Some examples of common rotational criteria; all the rotation senses are eastward. (A) Sheared and cracked garnets with asymmetric pressure shadows in pelitic schist, Mt. Kotsu nappe, Sakase. (B) Zoned amphibole at high angle to the schistosity plane, Bizan. (C) Asymmetric pressure shadows around garnet in glaucophane schist, South of Mt. Kotsu. (D) Pull-apart structure in epidote, basic schist, East of Omiko. (E) Sigmoidal biotite in pelitic schist with synthetic and antithetic shears, Sakase. (F) Pull-apart in pyroxene in gabbro, South of Shozanji.

Deformation regime

A comparative study of the rotational features in XY and YZ sections (i.e. respectively normal to the foliation plane and parallel or perpendicular to the L_1 lineation), has been undertaken at the outcrop, hand sample and thin-section scales, in order to test the hypothesis (based on the analysis of F_1 folds) that the deformation regime is rotational and the deformation can be explained by a shear mechanism along the L_1 trend. As a general result, in YZ sections (perpendicular to L_1) rotational features are scarce, and if present are inconsistent, so that no clear rotation sense can be determined (Fig. 12). In XZ sections (parallel to L_1), on the other hand, rotational features are conspicuous and consistent from the thin-section scale up to the outcrop one, regardless of rock type or metamorphic grade. Regionally a rotation sense from W to E is observed, parallel to the stretching and mineral lineation. Two exceptions giving rise to a westward rotation are noticed. They are related to the inverted limbs of the F_2 folds, especially along the second phase thrust at the base of the Mt. Kotsu nappe (Fig. 5), and around the F_3 upright folds where top and bottom must be carefully checked before sampling. On the mesoscopic scale, asymmetric quartz lenses (Fig. 15) in pelitic schists and sheared conglomerates are the most useful rotational criteria. The F_{1a} microfold asymmetry commonly shows an eastward overturning in agreement with other criteria. However, the overturning of sheath folds cannot be considered a reliable indicator of shear sense as the bedding polarity is unknown (e.g. Faure & Malavieille 1980, Mattauer *et al.* 1981).

Under the microscope, rotational criteria are conspicuous all over the infrastructure. The following well established criteria are used. (i) Asymmetric pressure shadows developed at the fringe of quartz and feldspar clasts in sandstone, pyroxene and pyrite grains in basic schist (Figs. 13 and 17), and garnet (Figs. 13 and 15), hornblende (Figs. 13 and 16) and albite porphyroblasts (Figs. 14 and 16) in high-grade metamorphic rock, are well-known non-coaxial strain markers (Fairbairn 1950, Zwart & Oele 1966, Choukroune 1971, Choukroune & Lagarde 1977, Mattauer *et al.* 1981). (ii) Oblique pull-apart structures that develop in minerals resistant to ductile deformation, such as pyroxene, epidote, piedmontite, and apatite (Fig. 13). Owing to the initial orientation of weak planes, both antithetic and synthetic slip with respect to the main shear plane are developed in agreement with computer simulation models (Etchecopar 1977) (Fig. 13). (iii) Sigmoidal phyllosilicates (Fig. 16) are reliable criteria for deriving the sense of shear (e.g. Eisbacher 1970, Choukroune & Lagarde 1977, Burg & Laurent 1978, Mattauer *et al.* 1981). (iv) Quartz deformation microstructures were also used as non-coaxial strain markers (Fig. 15). In SW Japan, their evolution follows that of the metamorphism, as temperature together with the strain rate are the main controlling parameters. In the southernmost part of the Shozanji nappe the radiolarites are weakly recrystallized, but in the Mt. Kotsu nappe they suffered syntectonic recrystallization shown by small grains with serrated boundaries surrounding large undulose clasts. Oblique subgrain

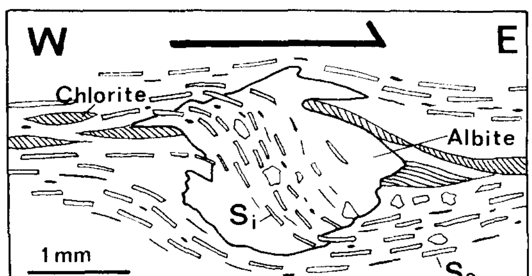

Fig. 14. Syntectonic albite porphyroblast with an internal schistosity (S_i) defined by epidote, amphibole, piedmontite, apatite, rutile and opaque minerals, branching into the matrix schistosity (S_e). S_i asymmetry agrees with an eastward rotation.

boundaries and internal shape fabric are in agreement with other rotational criteria (Brunnel 1980). Moreover, the *c*-axis lattice preferred orientations (LPO) display a monoclinic symmetry with a principal maximum at a small angle from the Z axis and a second one around the Y axis. Assuming that quartz deformation occurs by intracrystalline slip on the basal plane with some related slip on the prismatic plane the monoclinic LPO fabrics are due to non-coaxial deformation, as suggested by simulation models (Etchecopar 1977, Lister 1977). In the studied area the LPO diagrams show an eastward asymmetry, in agreement with other criteria observed in the same thin-section. (v) Sigmoidal inclusions in porphyroblasts should be used carefully. When there is evidence for syntectonic crystallization, such as continuity between internal (S_i) and external (S_e) schistosities, or the same mineralogical composition of the S_i and S_e schistosity, or S_i symmetry with respect to the center of the porphyroblast (e.g. Spry 1969, Schoneveld 1977, Vernon 1978), then the sigmoidal shape of S_i shows the rotation sense (Fig. 14). Assuming the porphyroblast behaves in the matrix as an isolated sphere in a Newtonian fluid, the shear strain γ is related to the S_i–S_e angle ω by: $2\omega = \gamma$. In our case γ averages 1.6 for amphibolite, but can reach 4 for some snow-ball garnets in glaucophane schist near Mt. Kotsu. However, such an evaluation is probably an underestimate. Albite spots in hornblende schist are generally zoned with an inclusion-rich core and an inclusion-free rim (Itaya 1978, Takagi & Hara 1979, Otsuki 1980). The rim develops asymmetrically along X and Y axes but never along Z. It is therefore interpreted as a kind of pressure shadow whose asymmetry is reliable with other non-coaxial criteria. In that case S_i orientation is highly variable even in one thin-section and its asymmetry does not allow a determination of rotation sense. Albite spots are also conspicuous in pelitic schist and quartz schist (Figs. 14 and 16). Pressure shadows at the end of these porphyroblasts are in agreement with an eastward rotation, but complexly folded inclusions do not provide reliable criteria.

INTERPRETATION AND CONCLUSION

The study of the first-phase deformation reveals that the structures are due to a rotational ductile shear with eastward displacement along the L_1 direction. The strain-ellipsoid measurements suggest a plane strain deformation. At the regional scale, during this deformation, the Greenschist nappes were thrust upon the Kurosegawa continent. Thus the L_1 lineation is a marker of nappe displacement direction: an 'a' kinematic lineation (e.g. Escher & Watterson 1974, Mattauer 1975, Mattauer *et al.* 1981). The infrastructure with its characteristic eastward ductile shear extends from Eastern Kyushu to North of Tokyo (Guidi *et al.* 1984) over more than 1000 km. Afterwards, the belt was refolded and reworked by longitudinal faults as the MTL or the Kurosegawa tectonic zone. The conspicuous bending observed in the Kanto area was caused by late Tertiary tectonics. Up to now the most popular geodynamic model, the "Pacific type orogeny" (Matsuda & Uyeda 1971), proposed for the Cenozoic deformations and extrapolated to the older orogenies (Miyashiro & Uyeda 1974), states that orogeny was due to subduction of oceanic crust under an island arc similar to the present Japanese Islands. Thus the HP/MT metamorphism is supposed to have been caused by subduction of an oceanic plate; but the nappe structures and the first phase ductile deformation are not considered in the model. Moreover a model based on progressive accretion of oceanic material along the southern margin of Japan does not account for the presence of pre-Triassic sialic rocks in the Kurosegawa zone. Collisional models have been already suggested to account for the Paleozoic metamorphic rocks in the Kurosegawa zone (Ichikawa 1981, Maruyama 1981) and for the paleomagnetic data (Sasajima 1982).

An explanatory model similar to those proposed for Corsica (Mattauer *et al.* 1977, Mattauer *et al.* 1981), the Western Alps (Caby *et al.* 1978, Mattauer & Tapponnier 1978), and the Himalayas (Mattauer 1975) where relationships between ductile deformation and large-scale tectonics are established, is suggested also for SW Japan. The basic assumption of the model is that the Jurassic orogeny of SW Japan was caused by the subduction of the Kurosegawa continent under an oceanic crust bearing the sediments of the Greenschist nappe, and by the resultant choking because continental crust cannot suffer very large amounts of subduction owing to its buoyancy. At depth the HP metamorphism and the ductile deformation occurred in the continental crust as well as in the overlying oceanic crust. The sediments were tectonically sliced and obducted upon the continental area. However, L_1 trends at about 25–30° from the general trend of the belt (Fig. 1), an orientation that is quite unusual when comparing with the other examples, where a displacement transverse to the regional trend is generally assumed. Thus in SW Japan, the convergent movement leading to the nappe tectonics was coupled with transcurrent movement subparallel to the chain. Strike-slip motion appears to be a striking feature of SW Japan, well established for the late Cretaceous (Ichikawa 1980), but it possibly began in Jurassic time as indicated by the ductile deformation. In addition to the ductile deformation described in this paper, the whole of SW Japan from the Japan Sea to the Kurosegawa zone suffered tangential tectonics at a more superficial structural level. A comprehensive model accounting for the Mesozoic history of SW Japan, involving sedimentation, metamorphism, deep and superficial tectonics, will be available after a geological survey of the superstructure, now in progress.

Acknowledgements—I would like to thank J. Charvet, A. Guidi, J. T. Iiyama, M. Iwasaki, M. Mattauer and K. Sano, for helpful suggestions and assistance at the various stages of the work. The research was financed by a grant of the Ministry of Education of Japan.

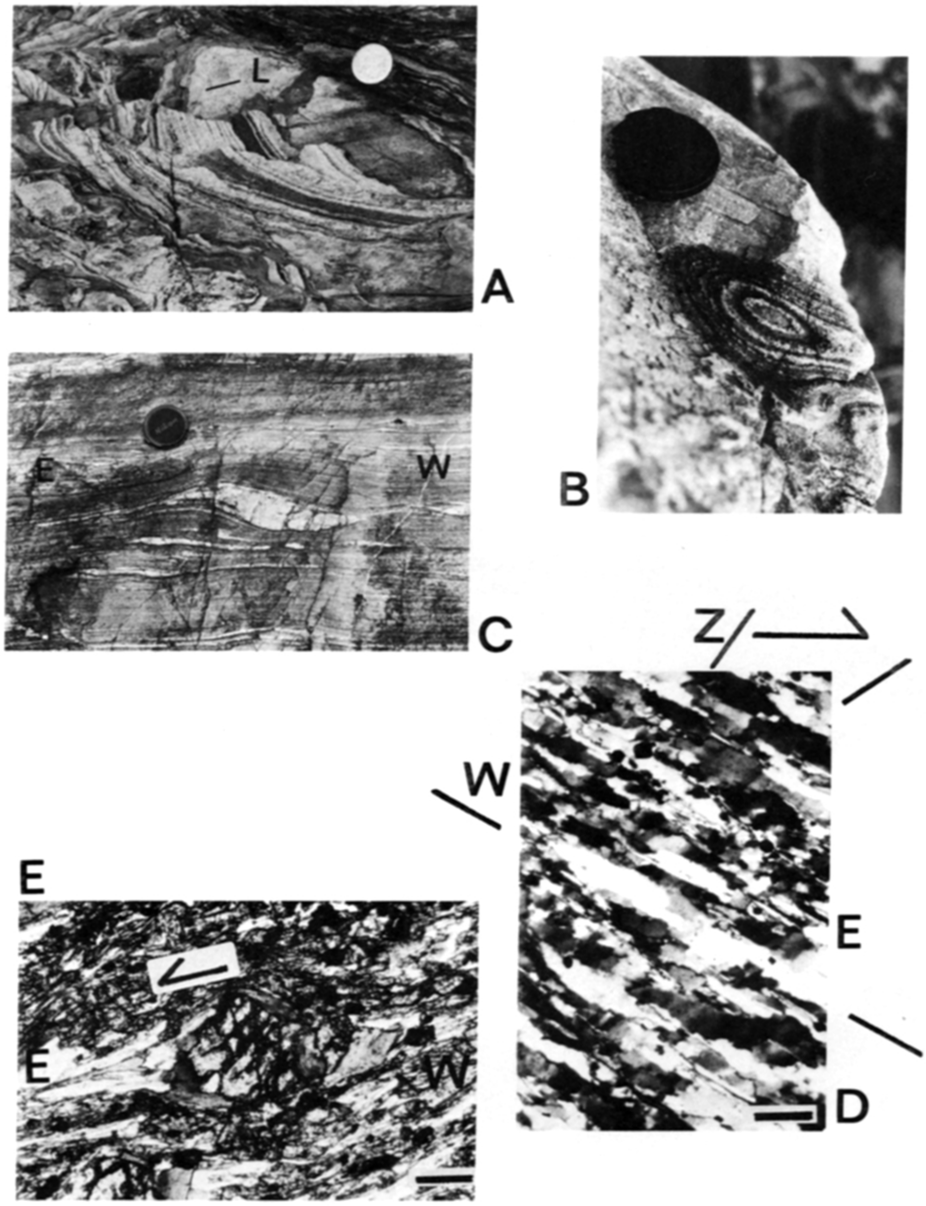

Fig. 15. (A) Curviplanar fold in the Oboke Unit (Omiko), with curved intersection lineation and constant mineral lineation L. (B) Eyed section of a sheath fold, perpendicular to the lineation, in calc schist of the Mt. Kotsu nappe, NW of Mt. Kotsu. (C) Asymmetric quartz lens in a pelitic schist of the Mt. Kotsu nappe, NE of Mt. Kotsu. (D) Quartzite (metaradiolarite?) in the Mt. Kotsu nappe (Sakase) showing oblique sub-grain structure and dynamic recrystallization. Scale bar is 1.3 mm. (E) Garnet with asymmetric chlorite pressure-shadows, Mt. Kotsu nappe east of Mt. Kotsu. Scale bar is 1.3 mm.

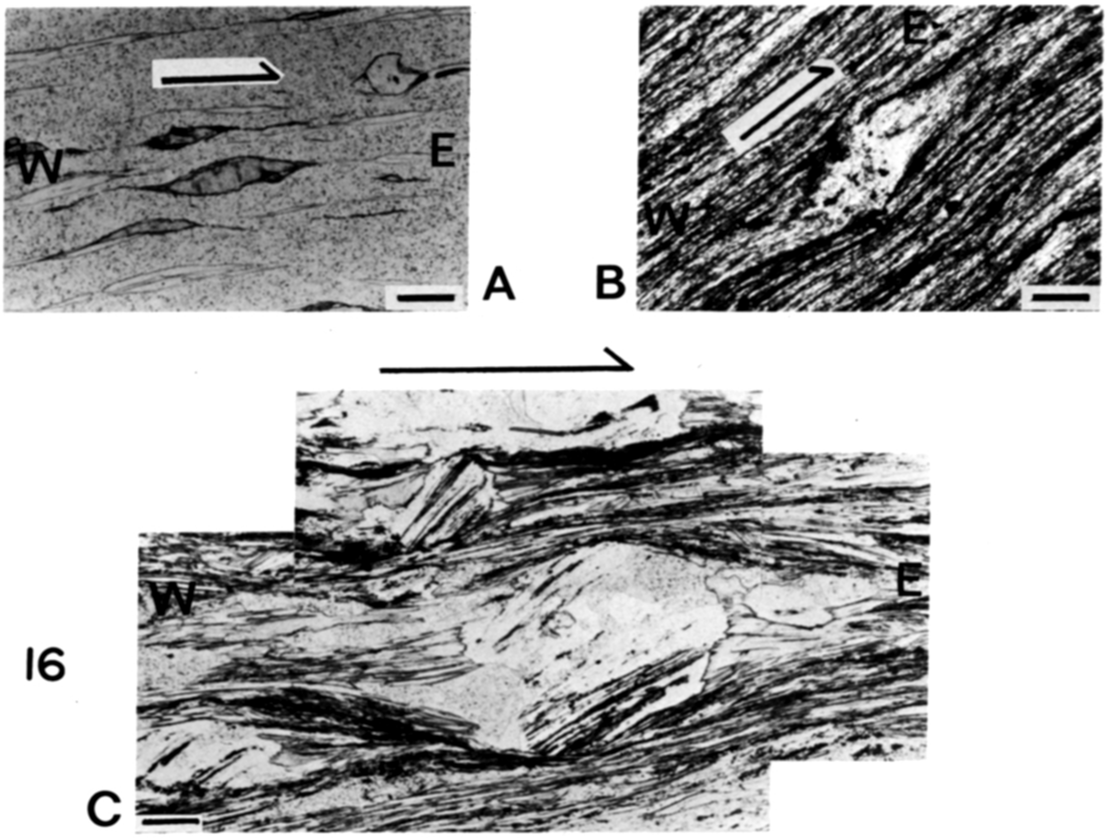

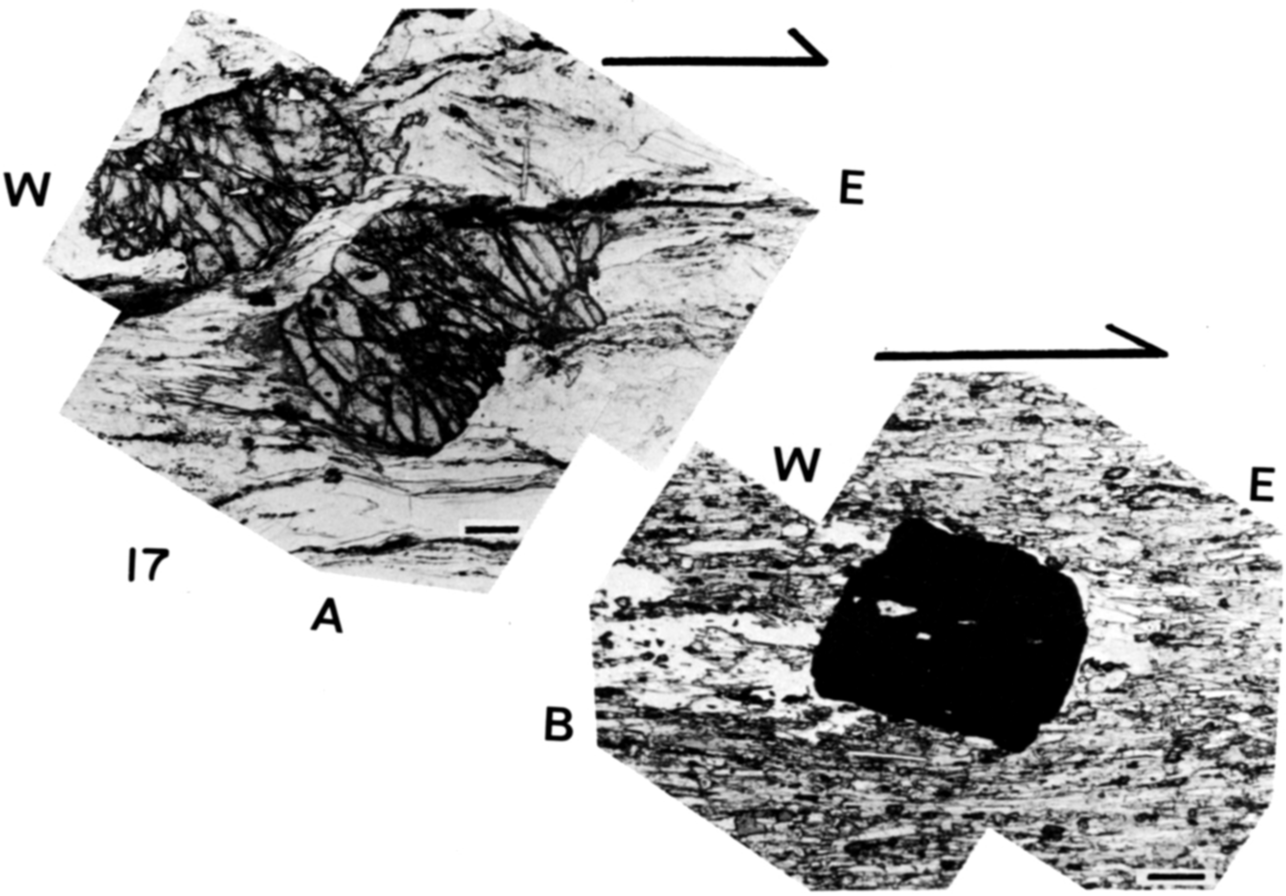

Fig. 16. Microphotographs of rotational criteria. The scale bar in each is 1.3 mm. (A) Sigmoidal amphibole (dark) and muscovite showing eastward asymmetry, Mt. Kotsu nappe, North of Sakase. (B) Asymmetric pressure shadows around clasts in shale, upper part of the Shozanji nappe, SE of Shozanji. (C) Asymmetric pressure shadow at the end of the albite porphyroblasts. The internal schistosity made up by opaque minerals is unrelated to the external one, Mt. Kotsu nappe, West of Bizan.

Fig. 17. (A) Sheared garnets with asymmetric pressure shadows; pelitic schist, Mt. Kotsu nappe, Sakase. (B) Opaque mineral with quartz pressure shadows in pelitic schist, Mt. Kotsu nappe, North of Mt. Kotsu.

REFERENCES

Banno, S. 1964. Petrologic studies on the Sanbagawa crystalline schists in the Besshi–Ino district, Central Shikoku, Japan. *J. Fac. Sci. Univ. Tokyo* Sec. 11, **15**, 203–356.

Banno, S., Higashino, T., Otsuki, M., Itaya, T. & Nakajuma, T. 1978. Thermal structures of the Sanbagawa belt in Central Shikoku. *J. Phys. Earth* **26**, 354–356.

Brunnel, M. 1980. Quartz *c*-axis fabrics in shear zone mylonites, evidence for a major imprint due to late strain increments. *Tectonophysics* **64**, T33–T44.

Burg, J. P. & Laurent, P. 1878. Strain analysis of a shear zone in a granodiorite. *Tectonophysics* **47**, 15–42.

Caby, R., Kienast, J. R. & Saliot, P. 1978. Structure, métamorphisme et modèle d'évolution tectonique des Alpes Occidentales. *Revue Géogr. phys. Géol. dyn.* **20**, 307–322.

Carreras, J., Estrada, A. & White, S. 1977. The effects of folding on the *c*-axis fabrics of a quartz mylonite. *Tectonophysics* **39**, 3–24.

Choukroune, P. 1971. Contribution à l'étude des mécanismes de la déformation avec schistosité grâce aux cristallisations syncinematiques dans les zones abritées (pressure shadows). *Bull. Soc. géol. Fr.* **7**, *Ser.* **13**, 257–271.

Choukroune, P. & Lagarde, J. L. 1977. Plans de schistosité et déformation rotationnelle: l'exemple des gneiss de Champtoceaux. *C. r. hebd. Séanc. Acad. Sci., Paris* **284**, 2331–2334.

Cobbold, P. & Quinquis, H. 1980. Development of sheath folds in shear regimes. *J. Struct. Geol.* **2**, 119–126.

Eisbacher, G. H. 1970. Deformation mechanics of mylonitic rocks and fractured granites at Cobequid Mountain, Nova Scotia, Canada. *Bull. geol. Soc. Am.* **81**, 2009–2020.

Ernst, W. G., Seki, Y., Onuki, H. & Gilbert, M. C. 1970. Comparative study of low grade metamorphism in the California Coast Ranges and the outer metamorphic belt of Japan. *Mem. geol. Soc. Am.* **124**, 1–276.

Escher, A. & Watterson, J. 1974. Stretching fabrics, folds and crustal shortening. *Tectonophysics* **22**, 223–231.

Etchecopar, A. 1977. Kinematic model of progressive deformation in polycrystalline aggregate. *Tectonophysics* **39**, 121–139.

Fairbairn, H. W. 1950. Pressure shadows and relative movements in a shear zone. *Trans. Am. geophys. Un.* **31**, 914–916.

Faure, M. 1982. Phase précoce Ouest–Est de la zone Sanbagawa dans la partie orientale de Shikoku. *C. r. hebd. Séanc. Acad. Sci., Paris* **295**, 505–510.

Faure, M. 1983. Eastward ductile shear during the early tectonic phase in the Sanbagawa belt. *J. geol. Soc. Japan* **89**, 319–329.

Faure, M. 1984. Schéma structural de la partie externe de la chaine mésozoique du Japon SW d'après l'exemple de l'ile de Shikoku. *C. r. hebd. Séanc. Acad. Sci., Paris* **298**.

Faure, M. & Malavieille, J. 1980. Les plis en fourreau du substratum de la nappe des schistes lustrés de Corse. Signification cinématique. *C. r. hebd. Séanc. Acad. Sci., Paris* **290**, 1349–1352.

Faure, M. & Charvet, J. 1983. Tangential tectonics in the Chichibu zone from the example of Eastern Shikoku. *Proc. Japan Acad.* **59** (B), **5**, 117–120.

Guidi, A., Charvet, J., Sato, T. & Takizawa, S. 1984. Les structures tangentielles anté-Crétacé dans les Monts Kanto: résultats préliminaires. *C. r. hebd. Séanc. Acad. Sci., Paris* **298**, 307–312.

Hada, S., Suzuki, T., Yoshikura, S. & Tsuchiya, N. 1979. The Kurosegawa zone in Shikoku and tectonic environment of the outer zone of southwest Japan. In: *The Basement of the Japanese Islands, Prof. H. Kano Mem. Vol.* Akita, 341–368.

Hara, I., Fujii, S., Nishimura, Y., Shiota, T. & Moriyama, K. 1973. Shape fabric of pebbles from the Oboke conglomerate schist. In: *Prof. Y. Umegaki Mem. Vol.* 103–111.

Hara, I., Hide, K., Takeda, K., Tsukuda, E. & Shiota, T. 1977. Tectonic movement in the Sanbagawa belt. In: *The Sanbagawa belt* (edited by Hide, K.), Hiroshima Univ. Press, 307–390.

Hide, K. 1961. Geologic structure and metamorphism of the Sanbagawa crystalline schists of the Besshi–Shirataki district in Shikoku, Southwest Japan. *Inst. Geol. Min. Fac. Sci., Hiroshima Univ. Rept.* **9**, 1–87.

Hide, K. 1972. Significance of the finding of two recumbent folds in the Sanbagawa metamorphic belt in the Ozu–Nagahama district. *Mem. Fac. Sci. Hiroshima Univ.* **3** (5), 35–51.

Hide, K., Yoshino, G. & Kojima, G. 1956. Preliminary report on the geologic structure of the Besshi spoted schists zone. *J. geol. Soc. Japan* **62**, 573–584.

Higashino, T. 1975. Biotite zone in the Sanbagawa metamorphic terrain in the Shiragayama area. Central Shikoku, Japan. *J. geol. Soc. Japan* **81**, 653–670.

Ichikawa, K. 1980. Geohistory of the Median Tectonic Line of Southwest Japan. *Mem. geol. Soc. Japan* **18**, 187–212.

Ichikawa, K. 1981. Closure of the Jurassic sea in and around the Ryoke–Sanbagawa Region (Abstract). In: *Tectonics of Paired Metamorphic Belts, Hiroshima Symposium* (edited by Hara, I.) 113–116.

Ichikawa, K., Ishii, K., Nakagawa, C., Suyari, K. & Yamashita, N. 1956. Die Kurosegawa zone. *J. geol. Soc. Japan* **62**, 82–103.

Itaya, T. 1978. Albite porphyroblasts containing retrograde TiO_2 minerals from the Sanbagawa pelitic rocks. *J. Japan. Ass. Min. Pet. Econ. Geol.* **73**, 339–345.

Iwasaki, M. 1963. Metamorphic rocks from the Kotu–Bizan Eastern Shikoku. *J. Fac. Sci. Univ. Tokyo* Sec. 11, **15**, 1–90.

Iwasaki, M. 1979. Gabbro breccia in the Mikabu greenstone belt of Eastern Shikoku. *J. geol. Soc. Japan* **85**, 481–487.

Kawachi, Y. 1968. Large-scale overturned structure in the Sanbagawa metamorphic zone in Central Shikoku. *J. geol. Soc. Japan* **74**, 607–616.

Kimura, T. 1973. The old inner arc of Japan and its deformation. In: *The Western Pacific, Island arcs, Marginal seas and Geochemistry* (edited by Coleman, P. J.). University of Western Australia Press, 255–273.

Kobayashi, T. 1941. The Sakawa orogenic cycle and its bearings on the origin of the Japanese islands. *J. Fac. Sci. Imp. Univ. Tokyo*, Sec. 11, **5**, 219–578.

Lagabrielle, Y., Auzende, J. M., Cornen, G., Juteau, T., Lensch, G., Mervel, C., Nicolas, A., Prichard, J., Ribeiro, A. & Vanney, J. R. 1982. Observations par submersible de la croûte océanique affleurant sur le banc de Gorringe: évidence de processus de démantèlement des gabbros en milieu sous-marin. *C. r. hebd. Séanc. Acad. Sci., Paris* **293**, 827–832.

Lister, G. 1977. Crossed girdle *c*-axis fabrics in quartzites plastically deformed by plane strain and progressive simple shear. *Tectonophysics* **39**, 51–54.

Maruyama, S. 1981. The Kurosegawa mélange zone and its role in the evolution of Southwest Japan. *Mem. geol. Soc. China* **4**, 269–279.

Matsuda, T. 1978. Discovery of the Middle–Late Triassic conodont genus "*Metapolygnathus*" from calcareous schists of the Sanbagawa southern marginal belt in Central Shikoku. *J. geol. Soc. Japan* **84**, 331–333.

Matsuda, T. & Uyeda, S. 1971. On the Pacific-type orogeny and its model extension of the paired belts concept and possible origin of marginal seas. *Tectonophysics* **11**, 5–27.

Mattauer, M. 1975. Sur le mécanisme de formation de la schistosité dans l'Himalaya. *Earth Planet. Sci. Lett.* **28**, 144–154.

Mattauer, M., Proust, F. & Etchecopar, A. 1977. Linéation "a" et mécanisme de cisaillement simple lié au chevauchement de la nappe des schistes lustrés en Corse. *Bull. Soc. géol. Fr.* 7 *Ser.* **14**, 841–847.

Mattauer, M. & Tapponnier, P. 1978. Tectonique des plaques et tectonique intracontinentale dans les Alpes franco-italiennes. *C. r. hebd. Séanc. Acad. Sci., Paris* **287**, 899–902.

Mattauer, M., Faure, M. & Malavieille, J. 1981. Transverse lineation and large-scale structures related to alpine obduction in Corsica. *J. Struct. Geol.* **3**, 401–409.

Miyashiro, A. 1961. Evolution of metamorphic belts. *J. Petrology* **2**, 277–311.

Miyashiro, A. & Uyeda, S. 1974. Plate tectonics and the Japanese Islands: a synthesis. *Bull. geol. Soc. Am.* **85**, 1159–1170.

Otsuki, M. 1980. Zonal structure of albite porphyroblasts from basic Sanbagawa schists in Central Shikoku. *Japan. J. Ass. Min. Petr. Ecol. Geol.* **75**, 196–202.

Quinquis, H., Audren, C., Brun, J. P. & Cobbold, P. 1978. Intensive progressive shear, in île de Groix blue schists and compatibility with subduction or obduction. *Nature, Lond.* **273**, 43–45.

Research group of the Sanbagawa belt, 1981. Tectonics of the Sanbagawa belt (Abstract). In: *Tectonics of Paired Metamorphic Belts. Hiroshima symposium* (edited by Hara, I.) 107–112.

Sasajima, S. 1982. Jurassic displacements inferred from paleomagnetism. *The Earth Monthly* **4**, 420–427.

Schoneveld, C. 1977. A study of typical inclusions patterns in strongly paracrystalline-rotated garnets. *Tectonophysics* **39**, 453–471.

Shiota, T. 1981. Structural, geological and petrological study of the Sanbagawa crystalline schists of the Ikeda–Mikamo district, East Shikoku. *J. Gakugei, Tokushima University* **32**, 29–65.

Spry, A. 1969. *Metamorphic Textures*. Pergamon Press, Oxford.

Suyari, K., Kuwano, Y. & Ishida, K. 1982. Stratigraphy and geological structure of the Mikabu green rocks Terrain and its environs. *J. Sci. Tokushima Univ.* **15**, 51–71.

Takagi, K. & Hara, I. 1978. Relationships between growth of albite porphyroblasts and deformation in a Sanbagawa schist, Central Shikoku, Japan. *Tectonophysics* **58**, 113–125.

Takasu, A. & Makino, K. 1980. Stratigraphy and geologic structure of the Sanbagawa metamorphic belt in the Besshi district, Shikoku, Japan. *Chikyu-kagaku* **34**, 16–26.
Tanaka, K. & Nozawa, T. 1977. *Geology and Mineral Resources of Japan. Geol. Surv. Japan.*
Toriumi, M. 1982. Strain, stress and uplift. *Tectonics* **1**, 57–72.
Vernon, R. H. 1978. Porphyroblast-matrix microstructural relationships in deformed metamorphic rocks. *Geol. Rdsch* **67**, 288–305.
Yokoyama, K. 1980. Nikubuchi peridotite body in the Sanbagawa metamorphic belt; thermal history of the "Al-pyroxene rich suite" peridotite body in high pressure metamorphic terrain. *Contr. Miner. Petrol.* **73**, 1–13.
Zwart, H. J. & Oele, J. A. 1966. Rotated magnetite crystals from the Rocroi Massif (Ardennes). *Geologie Mijnb.* **45**, 70–74.